Published online 8 November 2011

Nucleic Acids Research, 2012, Vol. 40, No. 5 ***2065–2075***
doi:10.1093/nar/gkr905

Specialization of an Exonuclease III family enzyme in the repair of 3′ DNA lesions during base excision repair in the human pathogen *Neisseria meningitidis*

Jan Silhan[1], Krzysztofa Nagorska[2], Qiyuan Zhao[1], Kirsten Jensen[1], Paul S. Freemont[1,*], Christoph M. Tang[2,3,*] and Geoff S. Baldwin[1,*]

[1]Division of Molecular Biosciences, [2]Centre for Molecular Microbiology and Infection, Imperial College London, South Kensington Campus, London, SW7 2AZ, UK and [3]Sir William Dunn School of Pathology, University of Oxford, South Parks Road, Oxford OX1 3RE, UK

Received July 22, 2011; Revised September 21, 2011; Accepted October 6, 2011

ABSTRACT

We have previously demonstrated that the two Exonuclease III (Xth) family members present within the obligate human pathogen *Neisseria meningitidis*, NApe and NExo, are important for survival under conditions of oxidative stress. Of these, only NApe possesses AP endonuclease activity, while the primary function of NExo remained unclear. We now reveal further functional specialization at the level of 3′-PO_4 processing for NExo. We demonstrate that the bi-functional meningococcal glycosylases Nth and MutM can perform strand incisions at abasic sites in addition to NApe. However, no such functional redundancy exists for the 3′-phosphatase activity of NExo, and the cytotoxicity of 3′-blocking lesions is reflected in the marked sensitivity of a mutant lacking NExo to oxidative stress, compared to strains deficient in other base excision repair enzymes. A histidine residue within NExo that is responsible for its lack of AP endonuclease activity is also important for its 3′-phosphatase activity, demonstrating an evolutionary trade off in enzyme function at the single amino acid level. This specialization of two Xth enzymes for the 3′-end processing and strand-incision reactions has not previously been observed and provides a new paradigm within the prokaryotic world for separation of these critical functions during base excision repair.

INTRODUCTION

Oxidative stress is one of the principle causes of DNA damage, and base excision repair (BER) is the main mechanism in living cells responsible for repairing the consequent DNA lesions. BER is therefore a well studied pathway in model organisms such as *Escherichia coli, Saccharomyces cerevisiae* and humans (1). Initially, damaged nucleobases are recognized and removed by DNA glycosylases, and the resulting apurinic/apyrimidinic (AP) sites, or incised products, are acted upon by the downstream AP endonucleases of the Exonuclease III (Xth) or Endonuclease IV (Nfo) family (2).

DNA glycosylases are responsible for recognizing and removing damaged DNA bases, and those involved in oxidative damage frequently remove multiple DNA lesions that can arise following oxidative damage (3). Glycosylases can also be bi-functional and incise the DNA backbone following removal of the base. The chemistry of these backbone incisions proceeds via an AP lyase activity in which base expulsion results from nucloephlilic attack of the 1′ of the ribose sugar, typically by the N-terminal amine or a lysine residue in the enzyme, with subsequent ring opening and strand cleavage occurring either via β-elimination to yield a 3′-unsaturated aldehyde (3′-Ald; Figure 1) or β-δ elimination leaving a 3′-phosphate (3′-PO_4; Figure 1) (4,5). These 3′-lesions cannot be repaired by a DNA polymerase and are therefore referred to as 3′-blocking lesions (2,6,7); such 3′-blocking lesions can also arise directly from oxidative damage leading to 3′-PO_4 and 3′-phosphoglycolate lesions (8). Further processing of these 3′-lesions typically occurs via the Xth or Nfo AP endonucleases to yield a 3′-OH that is competent for extension by a DNA polymerase (2,8).

*To whom correspondence should be addressed. Tel: +44 20 7594 5288; Fax: +44 20 7584 2056; Email: g.baldwin@imperial.ac.uk
Correspondence may also be addressed to Paul S. Freemont. Email: p.freemont@imperial.ac.uk
Correspondence may also be addressed to Christoph M. Tang. Tel: +44 1865 275560; Email: christoph.tang@path.ox.ac.uk

The authors wish it to be known that, in their opinion, the first two authors should be regarded as joint First Authors.

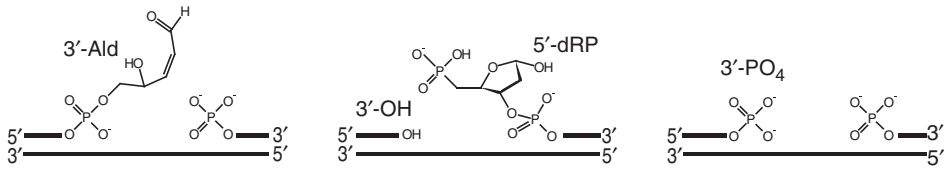

Figure 1. The intermediates of base excision repair. The different 3′-moieties generated during base excision repair. 3′-OH products are competent for further repair by DNA polymerase and ligase, while 3′–3′-Ald and 3′-PO_4 cannot be extended by DNA polymerase and are thus blocking lesions.

AP endonucleases are a critical component of BER since they also process AP sites that arise due to spontaneous base loss, or the action of monofunctional DNA glycosylases such as uracil DNA glycosylase (1,4). Incision of the DNA backbone at the abasic site is essential for further processing and repair, and AP endonucleases cleave 5′ to the AP site, leading to 3′-OH and 5′ deoxyribosephosphate (5′-dRP). This 5′ lesion must be processed by a deoxyribosephosphatase activity, and repair can then be effected by DNA polymerase and DNA ligase (1). The requirement for AP endonucleases to process both 3′-blocking lesions in addition to AP sites means these enzymes form a key node in BER, through which all lesions must pass en route to complete repair.

The Xth family of AP endonucleases are remarkably conserved across nature at the sequence and structural level (2,9–11). The *E. coli* ExoIII and human hAP1 enzymes form a four layered α/β sandwich structure with a binding pocket for the abasic deoxyribose that can accommodate the flipped out ribose in the enzyme-substrate complex (12,13). Both enzymes exhibit specific AP endonuclease cleavage in a Mg^{2+}-dependent manner (2). In addition, ExoIII has significant 3′–5′ exonuclease activity (14), although this is limited in hAP1 (15,16). Furthermore, both enzymes are able to process the 3′-Ald group (2,16,17) and ExoIII was initially described as a 3′-phosphatase (18), although this activity is significantly reduced in hAP1 (15). The Xth family of enzymes thus exhibit a wide range of biochemical activities and functions in living cells, although the exact complement and efficiencies of these reactions differ between specific enzymes (2).

We have previously demonstrated that, of the two Xth family enzymes in *Neisseria meningitidis*, only NApe possesses AP endonuclease activity (10). Although NExo exhibits a high degree of structural conservation with ExoIII and hAP1, it is the first example of this class of enzymes that is not a functional AP endonuclease. Despite this, both NApe and NExo make significant independent contributions to the ability of the meningococcus to withstand oxidative killing and to successful systemic bloodstream infection (10). The function of NExo is therefore a key unresolved issue in understanding the precise roles of the Xth family enzymes in meningococcal BER, as all its other activities (i.e. processing of 3′-Ald and 3′–5′ exonuclease) are also efficiently performed by NApe. Here, we sought to define the role of these Xth family enzymes, and the mechanisms employed by the meningococcus for processing AP sites and 3′-blocking lesions during BER.

MATERIALS AND METHODS

Construction of Neisserial strains

For the cloning of selected *N. meningitidis* genome fragments, DNA from strain MC58 (serogroup B) was used as a template in PCRs. Reactions were performed with Pfu polymerase (Promega) and appropriate primers. *Neisseria meningitidis* VPTL2 (*mutY*) was kindly provided by Dr Pelicic (Imperial College London). Details of all strains and plasmids are provided in Supplementary Table S1. To delete *nth, mutM, mutT*, *nexo*, *ung* and *tag*, the following strategy was employed. DNA fragments of between 650 and 1200 bp flanking the target gene were amplified by PCR with oligonucleotide primers; (primers detailed in Supplementary Table S2). The products were digested with appropriate restriction enzymes and ligated into pUC19 (19). Finally, antibiotic resistance genes were amplified from pDG1728 (for *spc*) (20) or pGCC4 (*erm*) (21) and inserted between the upstream and downstream fragments, generating the series of pDel plasmids (Supplementary Table S1), which were used to knock-out the target BER genes by a double-crossover recombination event. Transfromation of *N. meningitidis* MC58 resulted in replacing the target BER gene by an antibiotic marker due to exchanging of the complementary regions between the pDel plasmids and the chromosome. Transformants were analysed by PCR and western blotting to confirm that allelic replacement had occurred and that the protein was no longer expressed.

Bacterial survival assays under oxidative stress

Strains were grown on plates overnight, harvested into PBS and the bacterial suspensions adjusted to 10^9 colony-forming units (CFU)/ml. Subsequently, 100 µl of the bacterial suspension was incubated with 0.4 mM H_2O_2 (Sigma) for 30 min at room temperature. The same number of bacteria was incubated in PBS alone under the same conditions. After half an hour, serial dilutions were plated onto BHI medium. The number of CFU were counted the next day and the survival of each strain was expressed as the proportion of surviving bacteria after incubation with the oxidative agent(s) to the number recovered after incubation in PBS only. Assays were performed in triplicate on at least three independent occasions. Statistical significance was determined using a one-tail *t*-test.

Expression and purification of recombinant proteins

The gene for *mutM* (NMB1295) was amplified from MC58 using oligonucleotides MutMpET1 and

MutMpET2 (Supplementary Table S1) and the product inserted into pET-21a(+) using the NdeI and HindIII restriction sites in the primers. *Nth* (NMB0533) was amplified using oligonucleotides Nth1 and Nth2 (Supplementary Table S1) then ligated into pProEX-HTb (Invitrogen) using BamHI and HindIII. The terminating codon was added at the end of the *nth* gene using site-directed mutagenesis and oligonucleotides NthStop1 and NthStop2 (Supplementary Table S1). The final fusion protein contained an N-terminal polyhistidine tag with cleavage site for TEV protease. *Escherichia coli* Rosetta^{TM}(DE3) pLysS strain was used for protein expression.

Cultures for overexpression of Nth and MutM were typically grown in 3×500 ml of LB medium to an OD_{600} of 0.6 at 37°C, cooled to room temperature and then protein expression was induced by the addition of 0.5 mM IPTG, and growth continued at room temperature for a further 6 h. Cell pellets containing Nth were resuspended in PBS, 50 mM imidazole pH 8.0, 0.5 M NaCl and 2 mM β-mercaptoethanol (β-ME) and sonicated, while MutM pellets were resuspended in 2× PBS, 2 mM β-ME, 1 mM EDTA; sonicates were clarified by centrifugation. His-tagged Nth was purified on a metal affinity chromatography column loaded with Chelating Sepharose® Fast Flow (GE Healthcare) equilibrated charged with Ni^{2+} and equilibrated with PBS, 50 mM imidazole pH 8.0, 0.5 M NaCl and 2 mM β-ME. Nth protein was eluted with same buffer with 0.5 M imidazole. Fractions containing protein were pooled and purified on a HiLoad 26/60 GF Superdex75 column (GE Healthcare) equilibrated with buffer 25 mM Tris pH 7.5, 0.5 M NaCl and 2 mM β-ME. The polyhistidine tag was removed by overnight digestion by TEV protease (Invitrogen) at 4°C. Undigested Nth was removed on a Chelating Sepharose column while the remaining digested protein was dialysed against 25 mM Tris 7.5, 0.5 M NaCl, 1 mM EDTA, 2 mM DTT and 10% (v/v) glycerol. Clarified MutM lysates were subject to tandem anion/cation exchange chromatography on sequential columns filled with DE52 resin (Whatman Ltd) and SP Sepharose (GE Healthcare) on an ÄKTA purifier (GE Healthcare). The system was equilibrated with 20 mM Tris pH 7.5, 100 mM NaCl, 1 mM EDTA and 2 mM β-ME. After washing with the same buffer, MutM was eluted from the SP Sepharose column with a linear gradient of 1 M NaCl in the same buffer; protein eluted at ~375 mM NaCl. Fractions containing MutM were further purified using a HiLoad 26/60 GF Superdex75 column equilibrated 25 mM Tris 7.5, 0.5 M NaCl, 1 mM EDTA, 10% (v/v) glycerol and 2 mM β-ME.

NExo and NApe were obtained as described previously (10). *Escherichia coli* ExoIII was amplified from BL-21(DE3) and ligated into pET-21a(+) using the same strategy as for MutM. ExoIII was purified as for MutM. Human hAP1 lacking the first 35 amino acids (13) was expressed in *E. coli* and purified as for Nth.

DNA substrates, assays for DNA binding and AP lyase activity

All oligonucleotide substrates (Table 1 & Supplementary Table S4) were synthesized by Eurogentec and where necessary were further purified by HPLC, as previously described (22). Double-stranded DNA substrates were made by mixing equimolar amounts of complementary strands, heating to 90°C and cooling slowly to room temperature. Hairpin substrates were heated to 90°C and snap cooled on ice to facilitate intra-molecular annealing. Oligonucleotide binding was measured on a Fluoromax-3 fluorimeter monitoring both fluorescence anisotropy and intensity. In both cases, an excitation of 535 nm and emission at 556 nm was used. Binding assays were performed by titrating fixed concentrations of oligonucleotide (100 nM AP•G or C•G) with increasing amounts of enzyme at 25°C in binding buffer (50 mM Tris pH 7.5, 125 mM NaCl, 1 mM EDTA, 1 mM β-ME). Each protein titration was repeated three times; representative data are shown fitted to a combined binding equation for anisotropy and intensity using Scientist 3 (Micromath), full details are provided in Supplementary Figure S1 and Supplementary Table S3.

Table 1. DNA substrates

Name	Sequence
Uracil hairpin (U-hp)	5′-(HEX) GAC TAA UAA TGA CTG CGG TTA CGC AGT CAT TGT TAG TCT*T*T*T-3′
AP•G	5′-(HEX) GCT ATG GAC TAA (THF)AA TGA CTG CGT G-3′ CGA TAC CTG ATT G TT ACT GAC GCA C-5′
C•G	5′-(HEX) GCT ATG GAC TAA CAA TGA CTG CGT G-3′ CGA TAC CTG ATT GTT ACT GAC GCA C-5′
50-U	5′-(HEX) CGT GTA TGA CAT CTA ACT ATU ATA GCG CTC ATC GTC ATC GTC ATC CTC GGC ACC GT-3′ 3′-GCA CAT ACT GTA GAT TGA TAG TAT CGC GAG TAG CAG TAG CAG TAG GAG CCG TGG CA-5′
50-PO_4[a]	5′-(HEX) CGT GTA TGA CAT CTA ACT AT(PO_4) ATA GCG CTC ATC GTC ATC GTC ATC CTC GGC ACC GT-3′ 3′-GCA CAT ACT GTA GAT TGA TA G TAT CGC GAG TAG CAG TAG CAG TAG GAG CCG TGG CA-5′
20-PO_4	5′-(HEX) CGT GTA TGA CAT CTA ACT AT(PO_4) 3′-GCA CAT ACT GTA GAT TGA TA G TAT CGC GAG TAG CAG TAG CAG TAG GAG CCG TGG CA-5′
20-OH	5′-(HEX) CGT GTA TGA CAT CTA ACT AT 3′-GCA CAT ACT GTA GAT TGA TAG TAT CGC GAG TAG CAG TAG CAG TAG GAG CCG TGG CA-5′
ss20-OH	5′-(HEX) CGT GTA TGA CAT CTA ACT AT-3′
ss20-PO_4	5′-(HEX) CGT GTA TGA CAT CTA ACT AT (PO_4)-3′

THF is a tetrahydrofuran analogue; * is a methyl phosphonate linkage; U is deoxyuracil.
[a]Substrate 50-PO_4 was generated by enzymatic digestion of 50-U; see phosphatase assay for details.

Lyase activity was monitored with native abasic substrates generated by treating uracil containing oligonucleotides U-hp and 50-U with 5 nM hUDG (23) for 2 h to generate AP-hp and 50-AP respectively. The hairpin oligonucleotide was subsequently purified by gel filtration on a Superdex 75 column and concentrated with an Amicon ultra 3 k filter (Millipore); 50-AP oligonucleotides were used without further purification to avoid degradation. Steady-state reactions were initiated by mixing enzymes with substrates at a minimum ratio of 1:100 in reaction buffer (50 mM Tris pH 7.5, 125 mM NaCl, 1 mM EDTA, 1 mM β-ME and 0.1 mg/ml BSA) at 25°C; substrate concentrations were varied from 5 to 400 nM. Reactions were stopped at set time points in an equal volume of quench solution (0.01% xylene cyanol, 0.01% bromophenol blue, 40 mM EDTA in formamide), and separated by 20% denaturing PAGE. Gels were scanned on a fluorescence scanner FLA-5000 (Fuji), and quantified using Phoretix^{TM} 1D software. Initial velocities were determined by straight line fitting to the linear portion of the data. The initial velocities were corrected for enzyme concentration and the resulting reaction rates used to determine k_{cat} and K_m. Fitting was performed using Grafit 6 (Erithacus software).

Phosphatase and exonuclease assays

Double stranded 50-PO_4 was generated by treating 2 μM of annealed 50-U oligonucleotide with 50 nM hUDG (23) and 25 nM meningococcal MutM for 3 h. Digestion was verified by 20% denaturing PAGE and the 50-PO_4 substrate was used without further purification to avoid dissociation of the strands. 20-PO_4 and 20-OH were generated by annealing ss20-PO_4 or ss20-OH with an equimolar amount of complementary DNA. Reactions were initiated by mixing the enzyme with the substrate solution in exonuclease reaction buffer (50 mM Tris pH 7.5, 50 mM NaCl, 10 mM $MgCl_2$, 0.5 mM EDTA, 1 mM DTT and 0.1 mg/ml BSA) at 25°C, and quenched at specified time points as above, heated to 95°C for 5 min, cooled on ice, then separated on 20% denaturing PAGE and analysed as described above.

Nuclease assays with bacterial cell lysates

The bacteria-free extracts were obtained by spinning down 3 ml of O/N liquid culture and re-suspending the pellet in the mixture containing: 0.2 ml of BugBuster lysis buffer (Merck), 0.12 ml lysozyme (20 mg/ml) and protease inhibitor (Roche complete EDTA free) and gently agitating for 30 min at room temp. Once the solution was transparent, 0.8 ml of storage buffer [50 mM Tris pH 7.5, 500 mM NaCl, 1 mM EDTA and 50% (w/v) glycerol] was added and the sample spun down for 1 min (13 000 rpm) to remove the cell debris. Samples were stored at −20°C. The collected supernatant was used for activity assay with 20-PO_4 and 20-OH substrates. Reactions were carried out in exonuclease reaction buffer at 25°C, 20 μl of lysate corresponding to 1.5×10^8 CFU was mixed with 100 nM substrate in a 200 μl reaction for 60 min.

RESULTS

Contribution of BER enzymes to survival of *N. meningitidis* under oxidative stress

Initially we determined the contribution of all BER enzymes to survival of the meningococcus following exposure to oxidative stress. Strains were constructed with insertional mutations in genes encoding known or predicted BER enzymes, identified through biochemical or bioinformatics analyses (24,25). The level of survival of the mutants against the wild-type strain MC58 was compared after incubation in 0.4 mM H_2O_2 for 30 min before plating. Mutants deficient in the Nth and MutM enzymes, which are predicted to act against oxidative DNA lesions, do not exhibit any enhanced sensitivity as compared to those deficient in enzymes that act against the non-oxidative lesions 3-methyladenine (Tag) or uracil (Ung). However, it should be noted that oxidative conditions may increase rates of uracil deamination, and human UNG has been shown to have activity against minor oxidative lesions of cytosine (26,27). Data for NApe and NExo have here been measured with new strain deletions (Supplementary Table S1) and confirm our previous observations (10). These data emphasize the contribution of NApe and NExo to resistance against oxidative stress. Loss of NExo has the highest impact on bacterial survival with only 24% of the mutant surviving compared with the wild-type strain under the conditions tested ($P < 0.001$, Figure 2). This demonstrates that NExo has a critical role in bacterial survival during oxidative lesion repair, and must have a key function(s) within the meningococcus, distinct from the 3′-Ald activity that it shares with NApe (10).

Processing of abasic sites in *N. meningitidis*

Of the two Xth family members in *N. meningitidis*, only NApe has AP endonuclease activity (10). This single enzyme specialization is somewhat surprising given the overlapping activities frequently observed in other organisms, such as between ExoIII and EndoIV in *E. coli* (2). To fully evaluate the pathways for abasic site processing in the bacterium, we therefore investigated the two putative bi-functional DNA glycosylases, MutM and Nth identified in the genome (24). *Escherichia coli* MutM was initially named Fpg because formamidopyrimidine (FAPY) was its first characterized substrate (28,29). However, as the *E. coli* and meningococcal enzymes both recognize other DNA lesions including 8-oxoG (25,30), we refer to this enzyme as MutM (31). Nothing is known about the activity of the putative meningococcal Nth (encoded by NMB0533), which shares 72% amino acid identity with the *E. coli* enzyme that recognizes a broad range of oxidized pyrimidines (32). Potential AP lyase activity in these two enzymes means that they may act directly on abasic sites produced either by the action of mono-functional glycosylases or by direct depurination/depyrimidination following oxidative damage (33,34). Thus they may provide an alternative pathway for the processing of abasic sites, independent of NApe.

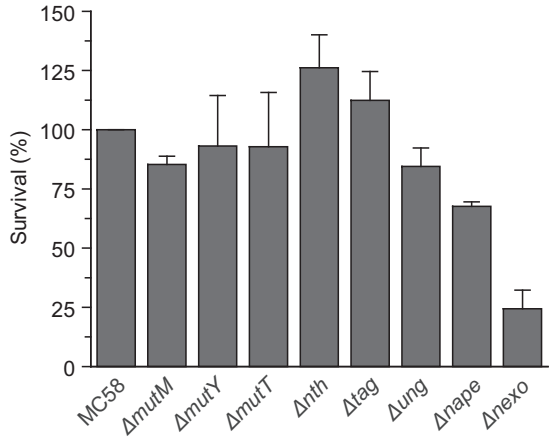

Figure 2. Contribution of individual BER enzymes to survival after exposure to oxidative stress. Mutant strains of all identified and putative BER enzymes in MC58 *N. meningitidis* were constructed and tested for survival under conditions of oxidative stress. Survival was calculated by comparing the number of bacteria recovered after treatment with 0.4 mM H_2O_2, or phosphate buffered saline, and shown as the percentage survival relative to the wild-type strain, MC58. Data shown are the mean of a minimum of three repeats with error bars to indicate the SD. Strains tested were deletions of: formamidopyrimidine DNA glycosylase (Δ*mutM*); adenine DNA glycosylase (Δ*mutY*); 8-oxoG nucleotide triphosphatase (Δ*mutT*); endonuclease III (Δ*nth*); 3-methyladenine DNA glycosylase (Δ*tag*); uracil N glycosylase (Δ*ung*); Neisserial AP endonuclease (Δ*nape*); Neisserial exonuclease (Δ*nexo*).

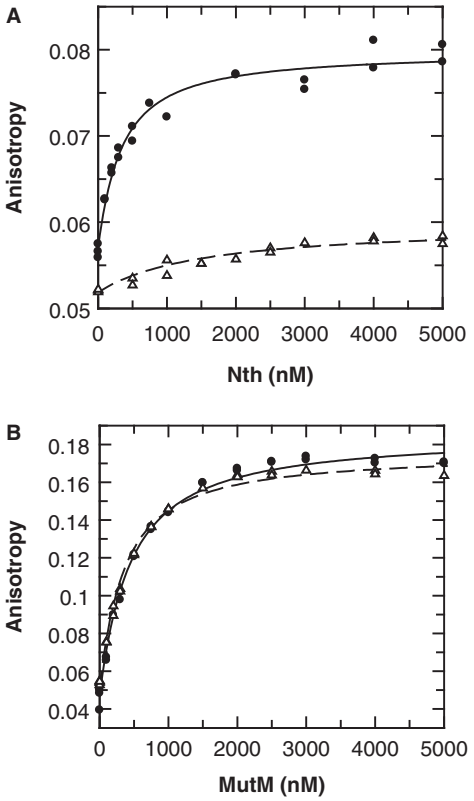

Figure 3. Binding of Nth and MutM to AP sites. Neisserial Nth and MutM enzymes were tested for binding to double-stranded 5′ HEX labelled oligonucleotides containing either an abasic furanose analogue or a non-specific sequence (AP•G and C•G, respectively; Table 1). Binding was determined by titrating increased amounts of enzyme into oligonucleotide (100 nM) and monitoring both fluorescence anisotropy and intensity. Binding of Nth lead to a significant decrease in HEX intensity that gives a distortion in the observed anisotropy (35): to compensate for this both anisotropy and intensity data were simultaneously fitted (Supplementary Figure S1), only anisotropy is shown here for clarity. (**A**) Binding of Nth is shown with the best fit to a single-site binding equation for AP•G (solid circles, K_d = 286 nM), and for C•G (open triangles, K_d = 1440 nM). (**B**) Binding of MutM is shown with the best fit to a single-site binding equation for AP•G (solid circles, K_d = 386 nM), and for C•G (open triangles, K_d = 303 nM).

To investigate this possibility, we examined the binding and lyase activities of the *Neisserial* MutM and Nth enzymes on AP sites and non-specific DNA. The meningococcal genes encoding MutM and Nth were cloned and expressed in *E. coli*, and the recombinant proteins purified to homogeneity (see 'Materials and Methods' section). Binding to AP sites was examined using double-stranded oligonucleotides containing an abasic furanose analogue, which cannot be cleaved by lyase activity (AP•G; Table 1), and a non-specific DNA (C•G; Table 1). The oligonucleotide was labelled at its 5′-end with HEX and binding monitored by fluorescence anisotropy and intensity. With MutM, there was no clear discrimination between the abasic DNA and a non-specific DNA. However, with Nth, a significant difference was observed with good binding to abasic DNA and only a relatively weak affinity to the non-specific oligonucleotide (Figure 3). Further to this, we also determined that there was no preference for binding to the abasic site, for either enzyme, when it was paired with either a G or an A (Supplementary Figure S1).

The lyase activity of Nth and MutM with a natural AP site was also examined and differences in gel migration clearly shows that the two enzymes yield products with different chemistry. Comparison with previous characterization of elimination products (33) demonstrates that Nth proceeds via β-elimination, generating a 3′-Ald, while MutM proceeds via β-δ elimination to yield a 3′-PO_4 (Figure 4A). Examination of the reaction profiles shows that the initial rates for both enzymes are very similar (Figure 4B and C). A steady state analysis of the enzymes demonstrated that they both had similar k_{cat} and K_m values (Figure 4D) but the reaction with MutM clearly does not proceed to completion and accumulation of product wanes as the reaction proceeds (Figure 4C and D). This can be explained by product inhibition; as the product accumulates it remains bound by the enzyme, reducing the availability of the enzyme to process substrates. Since steady-state rates are determined by the initial reaction velocity, product inhibition does not affect the determination of the k_{cat} and K_m of MutM.

3′-phosphatase and exonuclease activities of Xth family enzymes

Nicks and gaps in DNA that do not have 3′-OH groups are potentially highly cytotoxic to the meningococcus

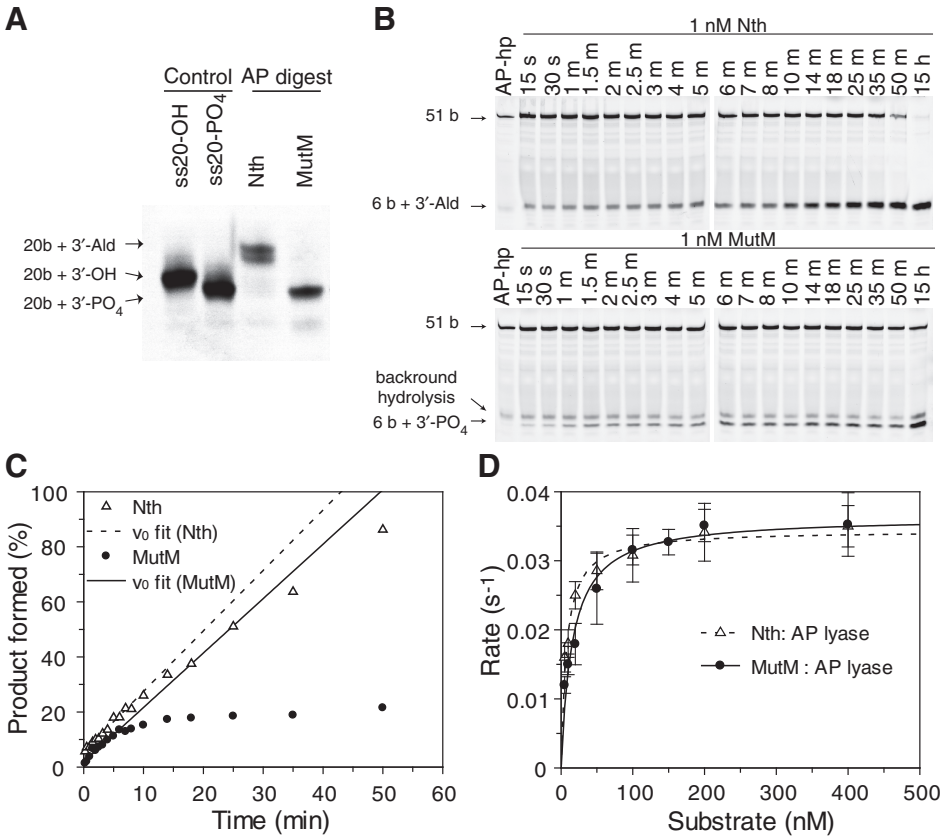

Figure 4. Cleavage of AP sites by Nth and MutM, and their products. (**A**) The products of Nth and MutM AP lyase activities were established by analysing reactions with the 50-AP substrate (see 'Materials and Methods' section) on a 20% denaturing polyacrylamide gel, and comparison with ss20-OH and ss20-PO_4 oligonucleotides. Observed migrations fit with those previously observed for 3′-Ald and 3′-PO_4 lesions (33), the dual band observed with the 3′-Ald is typical and likely due to different tautomers of the unsaturated aldehyde. (**B**) Typical steady-state reaction profiles are shown with AP-hp substrate (see 'Materials and Methods' section) for reactions with 1 nM Nth or MutM and 100 nM AP-hp substrate, showing accumulation of product over time. (**C**) Steady-state reactions were quantified by fluorescence scanning of gels, and the reaction profiles were fitted to a linear equation for the initial phase of the reaction; reactions with Nth (open triangles; dashed line) go to completion, while those for MutM (solid circles; solid line) are inhibited by product formation. (**D**) Steady-state analyses with AP-hp are shown with the best fit to the Michaelis–Menten equation for Nth (open triangles with a dashed line, $k_{cat} = 0.034 \pm 0.001$/s and $K_m = 7.5 \pm 1$ nM), and for MutM (solid circles with solid line, $k_{cat} = 0.036 \pm 0.002$/s and $K_m = 15.7 \pm 0.3$ nM). Error bars show the SD for experiments performed on a minimum of three occasions.

since they cannot be repaired by DNA polymerase and ligase. They thus present blocking lesions that hinder further downstream processing. We have previously demonstrated that both NApe and NExo can very efficiently remove 3′-Ald lesions (10). However, examination of the bi-functional DNA glycosylases present in *N. meningitidis* reveals that both 3′-PO_4 groups as well as 3′-Ald lesions are produced (Figure 4A). Since no enzyme has been identified that is responsible for the removal of 3′-PO_4 blocking lesions in the meningococcus, we investigated both NApe and NExo in relation to this activity. In addition, we performed the same assays on the well characterized ExoIII and HAP1 enzymes to provide a comparison of activities across the Xth family of enzymes.

Enzymes were incubated with a double stranded 50 bp oligonucleotide (50-PO_4; Table 1), which contained a 3′-PO_4 at an internal gap site generated by enzymatically by digestion of a uracil containing oligonucleotide with Ung and MutM. Oligonucleotides with a 3′-PO_4 migrate faster on PAGE than oligonucleotides of the same length with a 3′-OH, enabling monitoring of 3′-phosphatase activity (Figure 5A). Reaction aliquots were quenched at specific time points and resolved by denaturing PAGE; this was repeated with different concentrations of enzyme to observe the dynamic range of activities (Figure 5A–C). Even at the lowest enzyme concentration, it can be seen that NExo is the most efficient enzyme at removing the 3′-PO_4 to yield the 20-OH product, and is more active than ExoIII, for which this activity is well established (18,36). In comparison, neither NApe nor hAP1 show any 3′-phosphatase activity at this level of enzyme. As the concentration of enzyme was increased to 10 nM, the exonuclease activity of NExo and ExoIII can be seen to further degrade the DNA, and this occurs fastest for ExoIII. Even at the highest concentration of enzyme, the 3′-PO_4 is completely refractory to cleavage by NApe, although a small amount of 3′-phosphatase activity can be observed by hAP1 (Figure 5C).

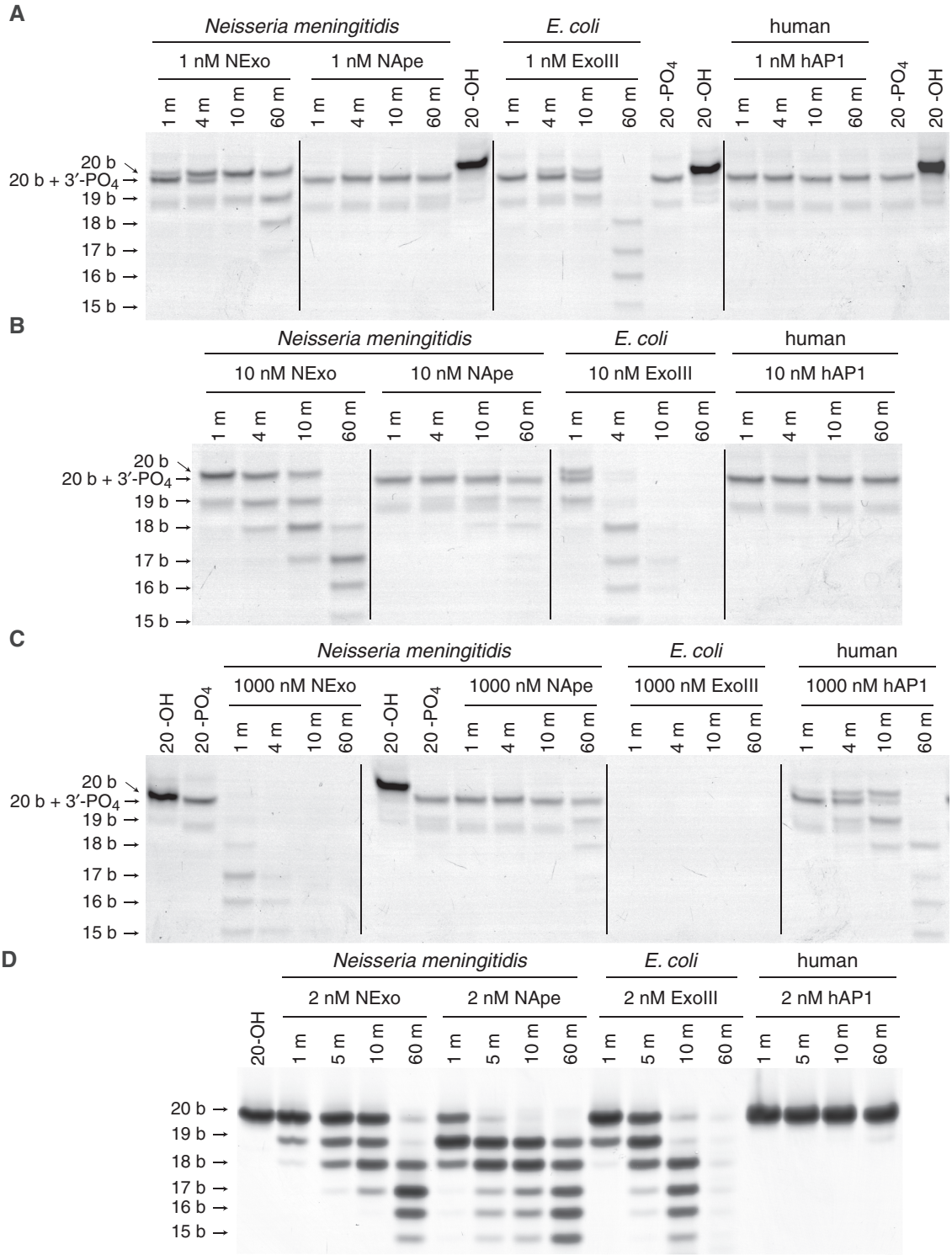

Figure 5. Comparative activity of Xth family endonucleases. Comparison of the 3′-phosphatase and 3′–5′ exonuclease activities of NExo, NApe, *E. coli* ExoIII and human hAP1. The substrates 50-PO_4 (100 nM; **A–C**) and 20-OH (200 nM; **D**) were incubated with different concentrations of enzyme as indicated under standard phosphatase assay conditions. Samples were taken at the time points indicated and the reactions quenched before separation by 20% denaturing PAGE.

Analysis of the 3′–5′ exonuclease activities of the enzymes reveals that ExoIII has the highest cleavage activity, NApe and NExo possess comparable activity, while hAP1 is clearly the slowest (Figure 5D). Moreover, this demonstrates that the inability of NApe and hAP1 to cleave the 3′-PO_4 substrate is unrelated to their exonuclease activities and highlights the blocking capacity of the 3′-PO_4 lesion, since it cannot be

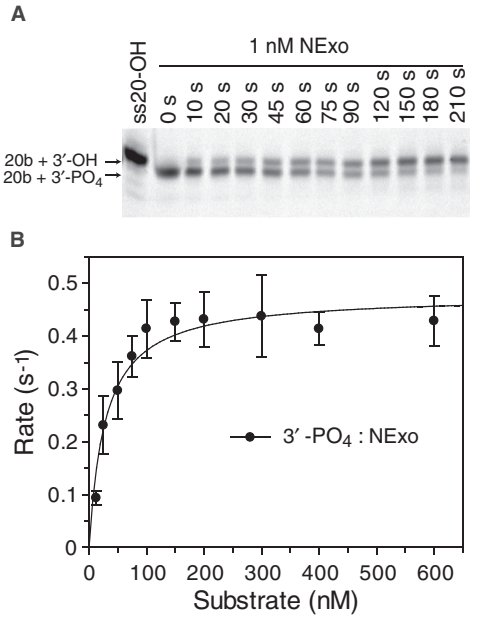

Figure 6. NExo is an efficient 3′-phosphatase. (**A**) 50-PO_4 (Table 1) was used as the substrate to measure removal of a 3′-blocking PO_4 from an internal AP site. NExo (1 nM) was incubated with 50-PO_4 (50 nM) under standard phosphatase assay conditions and aliquots removed at the indicated time points, quenched and resolved by denaturing 20% PAGE. (**B**) A number of reactions were performed with varying substrate concentrations using substrate 20-PO_4 (Table 1); quantified data are shown with the best fit to the Michaelis–Menten equation with $k_{cat} = 0.49 \pm 0.02$/s and $K_m = 28 \pm 6$ nM.

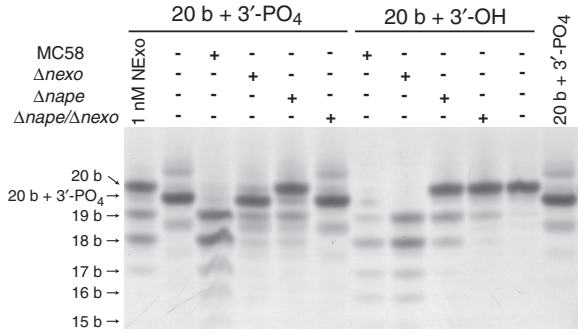

Figure 7. Cell extract activity. Cell lysates from wild type MC58, Δ*nape*, Δ*nexo* and Δ*nape*/Δ*nexo* strains were assayed for 3′-phosphatase, and 3′–5′ exonuclease activities. 100 nM substrate (20-PO_4 or 20-OH) was incubated with 10× diluted cell extracts from indicated strains under standard phosphatase/exonuclease assay conditions for 60 min. Products were separated by 20% denaturing PAGE.

bypassed through the exonuclease activity of the Xth enzymes.

Processing of 3′-PO_4 lesions by NExo

The above data indicated that NExo is able to process 3′-PO_4 lesions. We therefore characterized the kinetics of NExo against this specific lesion. To avoid enzyme pre-treatment synthetic 20-PO_4 substrate (Table 1) was used for Michaelis–Menten kinetics (both 20-PO_4 and 50-PO_4 substrates were processed with same rate; data not shown). It was notable that NExo exhibited highly efficient 3′-phosphatase activity, with a k_{cat} of 0.49/s (± 0.02) and K_m of 28 nM (± 6) (Figure 6B). Therefore, NExo is a highly efficient phosphatase that recognizes and removes blocking 3′-PO_4 lesion at internal gap sites and recessed 3′-termini.

NExo is the only 3′-phosphatase in *N. meningitidis*

Examination of the genome of MC58 did not reveal any other enzyme homologies, such as poly-nucleotide kinase (PNK), that may be associated with 3′-phosphatase activities. To determine whether NExo is the only enzyme with 3′-phosphatase activity, we assayed cell extracts from MC58, MC58Δ*nexo,* MC58Δ*nape* and MC58Δ*nexo*/Δ*nape* with the 20-PO_4 substrate (Figure 7). Extracts from the wild type meningococcus can clearly be seen to remove the 3′-phosphate with similar efficiency to 1 nM purified NExo, followed by rapid degradation through exonuclease activity. The NExo containing mutant extract (MC58Δ*nape*) matched the activity of the purified NExo enzyme with efficient 3′-phosphate processing, but reduced exonuclease activity. No 3′-phosphatase activity was observed with the MC58Δ*nexo* or MC58Δ*nexo*/Δ*nape* double mutant. Analysis of the 3′–5′ exonuclease activity with 20-OH substrate demonstrated that NAp and NExo account for all of the observed exonuclease activity in the cell extract. While both enzymes contribute to this, it is evident that NAp is responsible for the majority of exonuclease activity (Figure 7).

A key amino acid in NExo dictates its specificity

We have previously demonstrated that the activity of NExo is modulated by a His residue, which is a Ser or Gly in active AP endonucleases such as ExoIII and hAP1, respectively (10). This amino acid resides in the position that forms an abasic ribose binding pocket in the homologous human enzyme, hAP1 (10). The His residue thus sterically blocks recognition of the abasic site and modification to either Ser or Gly confers AP endonuclease activity to NExo (10). We therefore investigated whether this residue has an impact on 3′-PO_4 lesion processing by NExo. NExo $His^{167}Ser$ and $His^{167}Gly$ were both incubated with 20-PO_4 DNA containing a 3′-PO_4 lesion. Processing of the lesion was still observed with both mutants (Figure 8A–C). However, when the rate of 3′-phosphatase activity was determined it could be seen that both NExo $His^{167}Ser$ and $His^{167}Gly$ had ~10-fold lower activity than wild type (Figure 8C). Therefore, His^{167} is a critical residue for efficient 3′-PO_4 lesion processing by NExo.

DISCUSSION

The Neisserial exonuclease, NExo, is critical to the survival of the meningococcus under conditions of oxidative stress, since its removal has the most marked impact

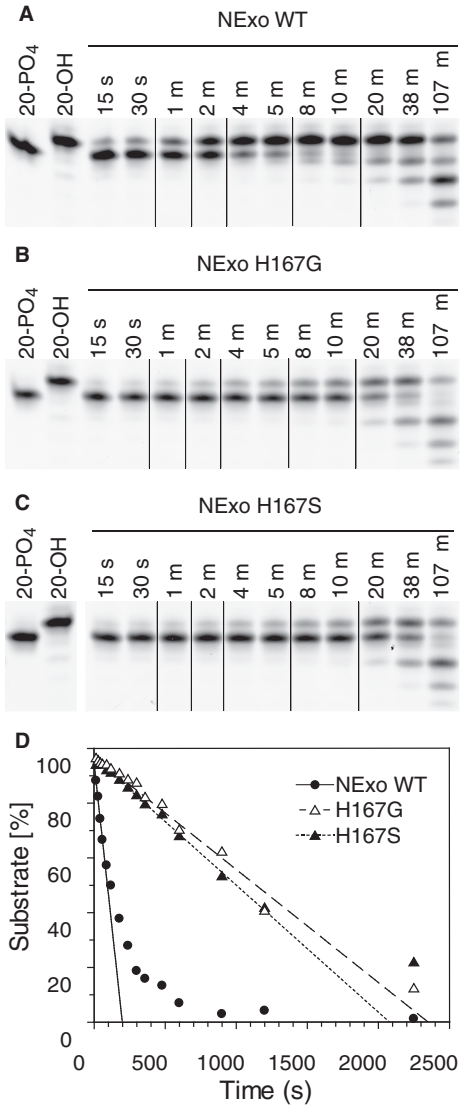

Figure 8. His^{167} is a key amino acid determining NExo activity. (**A–C**) Comparison of the phosphatase activity of NExo, NExo $His^{167}Gly$ and NExo $His^{167}Ser$ were performed by incubating 3 nM enzyme with 150 nM substrate 20-PO_4 under phosphatase assay conditions. Aliquots were removed at specified times, quenched and separated by 20% denaturing PAGE; representative lanes are shown for clarity. (**D**) Analysis of the full reaction profile is shown with fits to straight line plots to determine the initial velocity for NExo (solid circles, solid line; $k = 0.15$/s); NExo $His^{167}Gly$ (open triangles, dashed line; $k = 0.022$/s) and NExo $His^{167}Ser$ (closed triangles, dotted line; $k = 0.023$/s).

on bacterial survival compared with any other single component of the bacterium's BER system (Figure 1). Our previous studies have also highlighted the additive effect of deleting both NApe and NExo, indicating specialist roles for the enzymes (10). However, it was not evident what the distinct functions of these enzymes were within the bacterium. This is a key consideration since the Xth family of enzymes operate at a critical node in BER in the processing of AP sites and 3′-lesions (2,9,17), and we therefore investigated these activities within *N. meningitidis*.

The presence of only a single AP endonuclease, NApe, within the bacterium is unusual when compared to the *E. coli* and *S. cerevisiae* paradigms, which both have functional ExoIII and Nfo enzymes, both of which possess AP endonuclease activity (2). We determined that AP site processing can also be performed by the bi-functional DNA glycosylases Nth and MutM (Figure 3). Further to this, we characterized the 3′-lesions generated by Nth and MutM, which must be processed by the next stage of the BER pathway. Nth proceeds via β-elimination to produce a 3′-Ald, while MutM processes the lesion further, consistent with β-δ elimination to produce a 3′-PO_4 (Figure 4A). These chemistries are consistent with the reactions observed for this class of enzymes from other organisms (33,34,37,38).

It is therefore evident that both 3′-Ald and 3′-PO_4 lesions can arise either by the glycosylases-lyase action of Nth and MutM, or indeed by direct incision at abasic sites by these enzymes. Additionally, these lesions can form slowly by spontaneous β and subsequently δ-elimination or through hydrolysis of relatively unstable abasic sites that occur by spontaneous depurination and/or depyrimidination (39). Since both lesions present a block to repair by DNA polymerase, it is important to consider how they can be processed in the meningococcus.

We have here demonstrated that only NExo is able to process 3′-PO_4 lesions, and that this activity for NExo is more efficient than that of the well characterized *E. coli* ExoIII enzyme (Figure 5). In contrast, NApe is completely unable to cleave 3′-PO_4 lesions, a unique observation for this class of enzyme (Figure 5). When taken together with our previous observation that NApe is a highly efficient AP endonuclease, whereas NExo is completely resistant to processing of AP sites (10), we see extreme specializations for this family of enzymes within the meningococcus. Their activities are thus complementary and the balance of Xth family enzymes present in *N. meningitidis* represents a highly specialized solution to the processing of intermediates in BER.

A subpathway of BER in humans has previously been proposed that is independent of hAP1: the Nei-like enzymes, NEIL1 and 2 are bi-functional DNA glycosylases that incise the DNA backbone leaving 3′-PO_4 termini, which may then be processed by the 3′-phosphatase activity of polynucleotide kinase (PNK) (17). It has also been demonstrated that PNK is essential for rapid repair of single strand breaks under oxidative stress (40). *Escherichia coli* ExoIII can efficiently process all 3′-lesions (Figure 5), but the very slow 3′-PO4 processing observed with hAP1 (Figure 5) supports the proposal that hAP1 is not sufficiently active against 3′-phosphates to support this activity *in vivo* (17). The 3′-phosphatase activity of NExo is of particular relevance to *N. meningitidis*, since assays with cell extracts have confirmed that it is the only 3′-phosphatase activity in the meningococcus (Figure 7). Our data indicate that NExo serves an analogous role to PNK: steady-state reactions demonstrate that the kinetic constants for removal of 3′-PO_4 by NExo ($K_m = 28$ nM and $k_{cat} = 0.49$/s; Figure 6) are remarkably similar to values obtained for PNK ($K_m = 16$ nM and $k_{cat} = 0.46$/s) (17). Therefore,

NExo and PNK are members of unrelated protein families, yet strikingly share almost identical activity against 3′-PO4 lesions.

The importance of the 3′-phosphatase activity of NExo can be seen from the observed sensitivity of the MC58Δ*nexo* mutant under oxidative stress as compared to all other strains lacking single BER enzymes (Figure 1). 3′-PO_4 lesions are a blocking lesion that cannot be extended by DNA polymerase and since data from cell extracts demonstrate that NExo is the only enzyme in the meningococcus capable of processing this lesion, we conclude that 3′-phosphates are highly toxic to the cell and the loss of this activity largely accounts for the sensitivity of MC58Δ*nexo* to oxidative stress. It is also possible that NExo processes other lesions generated by direct strand cleavage from oxidative damage, which can also lead to 3′-blocking lesions such as 3′-glycolate (2) and which may contribute to the phenotypic sensitivity of MC58Δ*nexo*. The effect of this can be fully appreciated in the meningococcus, which not only has enzymes with a high degree of specialization, but also lacks an inducible SOS response that may otherwise mask the phenotype (24).

The data that we have presented here demonstrate that *N. meningitidis* possesses two Xth family enzymes that have evolved highly specific activities. The evolution of NExo to become a specialist 3′-end processing enzyme is evident from the critical His^{167} residue. We have previously shown that His^{167}Ser and His^{167}Gly modifications restore a significant degree of AP endonuclease activity to NExo (10). Here, we have shown that the same mutations reduce the efficiency of the 3′-phosphatase activity, demonstrating the evolutionary trade-off in activities that centres on this key amino acid (Figure 8). Although the structure of NExo provides insights into the mechanism by which His^{167} impairs AP endonuclease activity (10), it is not evident how the same residue contributes to its phosphatase activity. It is also notable that a mutation in the active site of HAP1 can increase its 3′-phosphatase and 3′-phosphodiesterase activities at the expense of AP site cleavage (41). There is thus a plasticity in this class of enzymes for the spectrum of activities that they possess, and in the case of both the Neisserial NExo and human HAP1 enzymes, broadening the range of activity reduces the efficiency of the specialized functions. This therefore points to the efficient 3′-phosphatase activity being a desirable evolutionary trait in this human pathogen, which has to survive persistent oxidative stress by the innate immune system during infection.

In conclusion, we have here defined the distinct roles for the two Xth family enzymes present in *N. meningitidis*: NExo is a specialized 3′-end processing enzyme, with sole activity against 3′-PO_4 lesions, while NApe is a specialized AP endonuclease. Although Nth and MutM may provide alternative pathways for strand incision, no such functional redundancy exists for 3′-PO_4 processing. These data demonstrate the importance of NExo in this pathogen, since it is required for efficient defence against oxidative stress, one of the primary responses of the host innate immune system to infection. This high degree of specialization between a pairing of Xth enzymes within an organism has not previously been observed and it is more frequent to have functional redundancy at this critical node in BER, even between enzymes of a different family, such as ExoIII and EndoIV in *E. coli* (2). Our previous bioinformatic study (10) suggests that this specialist enzyme pairing is widely dispersed within the prokaryotic world and it may present a new paradigm for separation of these two critical functions at the enzyme level.

SUPPLEMENTARY DATA

Supplementary Data are available at NAR Online: Supplementary Tables 1–4 and Supplementary Figure 1.

FUNDING

Programme Grants from the Wellcome Trust (084369/Z/07/Z) to P.S.F., G.S.B. and C.M.T. and the Medical Research Council to C.M.T. Funding for open access charge: Wellcome Trust.

Conflict of interest statement. None declared.

REFERENCES

1. Friedberg,E.C., Walker,G.C., Siede,W., Wood,R.D., Schultz,R.A. and Ellenberger,T. (2006) *DNA Repair and Mutagenesis*, 2nd edn. ASM Press, Washington, DC.
2. Demple,B. and Harrison,L. (1994) Repair of oxidative damage to DNA: enzymology and biology. *Annu. Rev. Biochem.*, **63**, 915–948.
3. Bjelland,S. and Seeberg,E. (2003) Mutagenicity, toxicity and repair of DNA base damage induced by oxidation. *Mutat. Res.*, **531**, 37–80.
4. O'Brien,P.J. (2006) Catalytic promiscuity and the divergent evolution of DNA repair enzymes. *Chem. Rev.*, **106**, 720–752.
5. Levin,J.D. and Demple,B. (1990) Analysis of class II (hydrolytic) and class I (beta-lyase) apurinic/apyrimidinic endonucleases with a synthetic DNA substrate. *Nucleic Acids Res.*, **18**, 5069–5075.
6. Boiteux,S. and Guillet,M. (2004) Abasic sites in DNA: repair and biological consequences in *Saccharomyces cerevisiae*. *DNA Repair*, **3**, 1–12.
7. Takemoto,T., Zhang,Q.M., Matsumoto,Y., Mito,S., Izumi,T., Ikehata,H. and Yonei,S. (1998) 3′-blocking damage of DNA as a mutagenic lesion caused by hydrogen peroxide in *Escherichia coli*. *J. Radiat. Res.*, **39**, 137–144.
8. Demple,B., Johnson,A. and Fung,D. (1986) Exonuclease III and endonuclease IV remove 3′ blocks from DNA synthesis primers in H2O2-damaged Escherichia coli. *Proc. Natl Acad. Sci. USA*, **83**, 7731–7735.
9. Parikh,S.S., Mol,C.D., Hosfield,D.J. and Tainer,J.A. (1999) Envisioning the molecular choreography of DNA base excision repair. *Curr. Opin. Struct. Biol.*, **9**, 37–47.
10. Carpenter,E.P., Corbett,A., Thomson,H., Adacha,J., Jensen,K., Bergeron,J., Kasampalidis,I., Exley,R., Winterbotham,M., Tang,C. *et al.* (2007) AP endonuclease paralogues with distinct activities in DNA repair and bacterial pathogenesis. *EMBO J.*, **26**, 1363–1372.
11. Demple,B., Herman,T. and Chen,D.S. (1991) Cloning and expression of APE, the cDNA encoding the major human apurinic endonuclease: definition of a family of DNA repair enzymes. *Proc. Natl Acad. Sci. USA*, **88**, 11450–11454.
12. Parikh,S.S., Mol,C.D. and Tainer,J.A. (1997) Base excision repair enzyme family portrait: integrating the structure and chemistry of an entire DNA repair pathway. *Structure*, **5**, 1543–1550.
13. Gorman,M.A., Morera,S., Rothwell,D.G., de La Fortelle,E., Mol,C.D., Tainer,J.A., Hickson,I.D. and Freemont,P.S. (1997) The crystal structure of the human DNA repair endonuclease

HAP1 suggests the recognition of extra-helical deoxyribose at DNA abasic sites. *EMBO J.*, **16**, 6548–6558.
14. Richardson,C.C., Lehman,I.R. and Kornberg,A. (1964) A deoxyribonucleic acid phosphatase-exonuclease from Escherichia coli. Ii. Characterization of the exonuclease activity. *J. Biol. Chem.*, **239**, 251–258.
15. Chen,D.S., Herman,T. and Demple,B. (1991) Two distinct human DNA diesterases that hydrolyze 3′-blocking deoxyribose fragments from oxidized DNA. *Nucleic Acids Res.*, **19**, 5907–5914.
16. Kane,C.M. and Linn,S. (1981) Purification and characterization of an apurinic/apyrimidinic endonuclease from HeLa cells. *J. Biol. Chem.*, **256**, 3405–3414.
17. Wiederhold,L., Leppard,J.B., Kedar,P., Karimi-Busheri,F., Rasouli-Nia,A., Weinfeld,M., Tomkinson,A.E., Izumi,T., Prasad,R., Wilson,S.H. *et al.* (2004) AP endonuclease-independent DNA base excision repair in human cells. *Mol. Cell.*, **15**, 209–220.
18. Richardson,C.C. and Kornberg,A. (1964) A deoxyribonucleic acid phosphatase-exonuclease from Escherichia coli. I. Purification of the enzyme and characterization of the phosphatase activity. *J. Biol. Chem.*, **239**, 242–250.
19. Yanisch-Perron,C., Vieira,J. and Messing,J. (1985) Improved M13 phage cloning vectors and host strains: nucleotide sequences of the M13mp18 and pUC19 vectors. *Gene*, **33**, 103–119.
20. Guerout-Fleury,A.M., Frandsen,N. and Stragier,P. (1996) Plasmids for ectopic integration in *Bacillus subtilis*. *Gene*, **180**, 57–61.
21. Mehr,I.J., Long,C.D., Serkin,C.D. and Seifert,H.S. (2000) A homologue of the recombination-dependent growth gene, rdgC, is involved in gonococcal pilin antigenic variation. *Genetics*, **154**, 523–532.
22. Grippon,S., Zhao,Q., Robinson,T., Marshall,J.J., O'Neill,R.J., Manning,H., Kennedy,G., Dunsby,C., Neil,M., Halford,S.E. *et al.* (2010) Differential modes of DNA binding by mismatch uracil DNA glycosylase from *Escherichia coli*: implications for abasic lesion processing and enzyme communication in the base excision repair pathway. *Nucleic Acids Res.*
23. Krusong,K., Carpenter,E.P., Bellamy,S.R., Savva,R. and Baldwin,G.S. (2006) A comparative study of uracil-DNA glycosylases from human and herpes simplex virus type 1. *J. Biol. Chem.*, **281**, 4983–4992.
24. Davidsen,T. and Tonjum,T. (2006) Meningococcal genome dynamics. *Nat. Rev. Microbiol.*, **4**, 11–22.
25. Tibballs,K.L., Ambur,O.H., Alfsnes,K., Homberset,H., Frye,S.A., Davidsen,T. and Tonjum,T. (2009) Characterization of the meningococcal DNA glycosylase Fpg involved in base excision repair. *BMC Microbiol.*, **9**, 7.
26. Dizdaroglu,M., Karakaya,A., Jaruga,P., Slupphaug,G. and Krokan,H.E. (1996) Novel activities of human uracil DNA N-glycosylase for cytosine-derived products of oxidative DNA damage. *Nucleic Acids Res.*, **24**, 418–422.
27. An,Q., Robins,P., Lindahl,T. and Barnes,D.E. (2005) C –> T mutagenesis and gamma-radiation sensitivity due to deficiency in the Smug1 and Ung DNA glycosylases. *EMBO J.*, **24**, 2205–2213.
28. Chetsanga,C.J. and Lindahl,T. (1979) Release of 7-methylguanine residues whose imidazole rings have been opened from damaged DNA by a DNA glycosylase from *Escherichia coli*. *Nucleic Acids Res.*, **6**, 3673–3684.
29. Boiteux,S., Bichara,M., Fuchs,R.P. and Laval,J. (1989) Excision of the imidazole ring-opened form of N-2-aminofluorene-C(8)-guanine adduct in poly(dG-dC) by *Escherichia coli* formamidopyrimidine-DNA glycosylase. *Carcinogenesis*, **10**, 1905–1909.
30. Morland,I., Rolseth,V., Luna,L., Rognes,T., Bjoras,M. and Seeberg,E. (2002) Human DNA glycosylases of the bacterial Fpg/MutM superfamily: an alternative pathway for the repair of 8-oxoguanine and other oxidation products in DNA. *Nucleic Acids Res.*, **30**, 4926–4936.
31. Nghiem,Y., Cabrera,M., Cupples,C.G. and Miller,J.H. (1988) The mutY gene: a mutator locus in *Escherichia coli* that generates G.C—T.A transversions. *Proc. Natl Acad. Sci. USA*, **85**, 2709–2713.
32. Dizdaroglu,M., Laval,J. and Boiteux,S. (1993) Substrate specificity of the *Escherichia coli* endonuclease III: excision of thymine- and cytosine-derived lesions in DNA produced by radiation-generated free radicals. *Biochemistry*, **32**, 12105–12111.
33. Bailly,V., Verly,W.G., O'Connor,T. and Laval,J. (1989) Mechanism of DNA strand nicking at apurinic/apyrimidinic sites by *Escherichia coli* [formamidopyrimidine]DNA glycosylase. *Biochem. J.*, **262**, 581–589.
34. Ikeda,S., Biswas,T., Roy,R., Izumi,T., Boldogh,I., Kurosky,A., Sarker,A.H., Seki,S. and Mitra,S. (1998) Purification and characterization of human NTH1, a homolog of *Escherichia coli* endonuclease III. Direct identification of Lys-212 as the active nucleophilic residue. *J. Biol. Chem.*, **273**, 21585–21593.
35. Bellamy,S.R., Krusong,K. and Baldwin,G.S. (2007) A rapid reaction analysis of uracil DNA glycosylase indicates an active mechanism of base flipping. *Nucleic Acids Res.*, **35**, 1478–1487.
36. Rogers,S.G. and Weiss,B. (1980) Exonuclease III of *Escherichia coli* K-12, an AP endonuclease. *Methods Enzymol.*, **65**, 201–211.
37. Bailly,V. and Verly,W.G. (1987) Escherichia coli endonuclease III is not an endonuclease but a beta-elimination catalyst. *Biochem. J.*, **242**, 565–572.
38. Nash,H.M., Bruner,S.D., Scharer,O.D., Kawate,T., Addona,T.A., Spooner,E., Lane,W.S. and Verdine,G.L. (1996) Cloning of a yeast 8-oxoguanine DNA glycosylase reveals the existence of a base-excision DNA-repair protein superfamily. *Curr. Biol.*, **6**, 968–980.
39. Lindahl,T. (1993) Instability and decay of the primary structure of DNA. *Nature*, **362**, 709–715.
40. Breslin,C. and Caldecott,K.W. (2009) DNA 3′-phosphatase activity is critical for rapid global rates of single-strand break repair following oxidative stress. *Mol. Cell. Biol.*, **29**, 4653–4662.
41. Castillo-Acosta,V.M., Ruiz-Perez,L.M., Yang,W., Gonzalez-Pacanowska,D. and Vidal,A.E. (2009) Identification of a residue critical for the excision of 3′-blocking ends in apurinic/apyrimidinic endonucleases of the Xth family. *Nucleic Acids Res.*, **37**, 1829–1842.